mathematics

MDPI

Article

Pareto Optimization of Energy-Saving Timetables Considering the Non-Parallel Operation of Multiple Trains on a Metro Line

Weiya Chen [1,2,*], Jiaqi Lu [1,2], Hengpeng Zhang [1] and Ziyue Yuan [1,2]

[1] School of Traffic and Transportation Engineering, Central South University, Changsha 410075, China; 204212087@csu.edu.cn (J.L.); 184211030@csu.edu.cn (H.Z.); zyyuan@csu.edu.cn (Z.Y.)
[2] Rail Data Research and Application Key Laboratory of Hunan Province, Changsha 410075, China
* Correspondence: wychen@csu.edu.cn

Abstract: In light of reducing train operation energy consumption while maintaining the passenger service level for creating sustainable urban rail transit systems, we address a non-parallel train timetabling problem considering regenerative braking energy utilization and the non-parallel operation of multiple trains on a metro line via a newly proposed multi-objective timetable (MOT) optimization model and an evolutionary algorithm based on NSGA-II. The optimization objectives of the MOT model are to find satisfactory energy-saving timetables on the Pareto frontier by minimizing the total travel time of passengers and minimizing the net energy consumption of trains. An improved multi-objective evolutionary algorithm based on NSGA-II is constructed to generate the optimal arrival and departure times at each station for each train running in a non-parallel operation mode. This study tests the feasibility of the proposed optimization method via an empirical case using the data collected from the Yizhuang Line of the Beijing metro systems in China. The simulation results show that the proposed optimization method satisfies both the energy utilization and passenger service levels along a Pareto front. The MOT improves the overall effectiveness of regenerative braking energy utilization by 29.88% in comparison with the original timetable; it reduces the net operation energy consumption by 44.86% relative to the travel-oriented timetable (TOT); and it reduces the total passenger travel time by 27.18% compared with the energy-oriented timetable (EOT).

Keywords: metro; non-parallel operation of multiple trains; energy-saving timetable; NSGA-II algorithm; regenerative braking energy

MSC: 90B06

check for updates

Citation: Chen, W.; Lu, J.; Zhang, H.; Yuan, Z. Pareto Optimization of Energy-Saving Timetables Considering the Non-Parallel Operation of Multiple Trains on a Metro Line. *Mathematics* **2023**, *11*, 4491. https://doi.org/10.3390/math11214491

Academic Editors: Chin-Chia Wu, Win-Chin Lin, Jatinder N. D. Gupta and Xingong Zhang

Received: 30 September 2023
Revised: 25 October 2023
Accepted: 29 October 2023
Published: 30 October 2023

1. Introduction

Cities identify urban rail transit as a service complementary to other sustainable forms of urban public transit systems. More generally, designing low-carbon urban rail transit systems is a critical component of reducing emissions and addressing climate change at the urban scale [1]. Daily operations account for more than 90% of total greenhouse gas (GHG) emissions throughout the entire life cycle of a metro [2]. Major energy-saving enhancements for urban rail transit thus aim to improve the operational energy performance. Theoretical investigations primarily focus on operational energy-saving approaches, such as trajectory control strategies (e.g., optimizing the operation time between stations [3], departure/arrival times [4], dwell and running times of a train [5,6], and speed profiles [7]) and energy storage systems (e.g., the utilization of regenerative braking technology [8]). The efficiency of trajectory control strategies is mostly restricted by the safety distance between trains and the stability of the power grid. Regenerative braking technology can save an appropriate percentage of energy consumption (around 33% in the traction energy flow [9]). The energy transfer [10,11] and utilization efficiency [12] of regenerative braking are widely considered to minimize energy loss during braking. Meanwhile, some studies have explored the voltage-stabilizing effects and aim to enhance the efficiency of energy storage systems directly [13]. The increasing number of urban rail transit systems under development have made it even more essential to design measures for systematically reducing operational energy consumption levels.

In urban rail transit systems, energy usage is typically classified as traction or non-traction consumption activities. The energy required to operate rolling stock (i.e., trains) within the system is referred to as traction energy consumption [9], and accounts for more than 50% of the energy consumption of metro operations [11]. Previous studies primarily focused on different energy-saving strategies targeted at traction consumption by optimizing train speed profiles or timetables, both with and without regenerative braking functions. With regenerative braking, the energy produced during the braking process can be recovered and reused, resulting in a reduction in the overall energy consumption [14]. In addition, different types of trains have adopted distinct control conditions in different environments (e.g., the optimal utilization of the gravitational potential energy generated by a train when moving downhill [15]) to further reduce energy consumption levels.

The optimization of train timetables, meanwhile, mainly considers the overlap between the traction and braking phases and the duration of the running time [16,17]. The existing research also focuses on energy-saving operational strategies and timetable optimization methods based on parallel operation diagrams. The rapid development of urban rail transit systems makes train operations more complex and the utilization of non-parallel operation diagrams more frequent. Previous studies have focused on energy-saving operational strategies and timetable optimization based on parallel train operation diagrams but have overlooked the further utilization of non-parallel operation diagrams in the development of urban rail transit systems. Under non-parallel operation diagrams, the complexity of passenger flows and non-parallel train running features create significant challenges for train scheduling. To further explore non-parallel train operations, this study proposes an energy-saving-based non-parallel operation timetable optimization method with a multi-objective timetable (MOT) optimization model with considerations of both the passenger service level and train operation energy consumption and an improved multi-objective evolutionary algorithm based on NSGA-II. This study then tests the feasibility of the proposed energy-saving timetable optimization method via an empirical case.

In summary, this study proposes an energy-saving timetable optimization method under non-parallel operation diagrams with more complex passenger demands. Secondly, the proposed MOT optimization model aims to minimize both the net operational energy consumption and total passenger travel time. Thirdly, the proposed optimization approach provides a theoretical basis for designing an energy-saving urban rail transit system.

2. Literature Review

Energy-saving operational strategies have been investigated in two major ways: the utilization of the potential gravitational energy of a train [15] and the flexibility of control conditions [18]. These investigations were conducted both with and without considering the implementation of regenerative braking technology. Prior to the implementation of regenerative braking technology, previous conventional studies focused on optimizing operations and reducing energy consumption levels based on the characteristics of individual track sections. He et al. (2015) optimized the train speed profiles of each inter-station line segment through a section separation analysis by incorporating both running line-related features [19]. Deng et al. (2021) considered the predetermined running times for each inter-station track segment and optimized the control condition sequences and durations along each section by regulating the multi-speed parameters [18]. Meanwhile, some studies explore the design of timetables that optimize the overlap times of control conditions between adjacent trains, thereby enhancing the utilization efficiency of regenerative braking energy. Sun et al. (2017) optimized the sequence of control conditions for adjacent trains [20]; Bai et al. (2020) investigated the application of the secondary traction of the train when optimizing the control conditions of a single train in the section [21,22].

An alternate approach to energy saving is schedule optimization, particularly prior to the implementation of regenerative braking technology. He et al. (2021) proposed a two-stage energy-saving calculation method to globally optimize the allocation of total train running times between different sections [23]. Gao et al. (2020) optimized the allocation of inter-station running times by calculating the optimal control strategy for inter-station train operations along a Pareto frontier [24]. When regenerative braking technology was implemented, many previous studies focused on optimizing the temporal and spatial elements of parallel operation diagrams to minimize energy consumption levels and design optimal timetables. Peng et al. (2017) used the controllability of train headway and dwell times to minimize the total energy consumption [10]. Ran et al. (2020) assumed that train headway and turnaround times were fixed, and then moderately optimized the dwell time, inter-station running time, and turnaround time so as to minimize the net energy consumption [25]. Wei et al. (2020) considered the overlapping time distribution and distance between the front and rear trains, and then optimized the arrival, departure, and dwell times of trains traveling in the same direction [12].

While reducing operational energy consumption levels, it is also critical to consider other factors, especially passenger demands. He et al. (2020) developed an integrated optimization method to minimize both the energy consumption and transfer waiting time cost for transfer passengers [3]. Wu et al. (2020) designed a multi-objective timetabling optimization and incorporated the consideration of the crowdedness of passengers [26]. Xie et al. (2021) proposed an energy-saving timetable for a high-speed railway line, meanwhile avoiding time delays for passengers [5].

The existing research mainly focuses on the energy-saving operations and timetable optimizations under train parallel operation diagrams. In light of the more and more complex train speed profiles and increasing passenger demands, non-parallel train operation diagrams are crucial for address rapid urban rail system developments. Non-parallel operation diagrams introduce increased complexity in terms of the running features of trains and the characteristics of passenger flows. To further explore the use of non-parallel operation diagrams, this study aimed to establish an energy-saving timetable optimization method.

3. Optimization Model

A metro line is depicted as the domain of $\mathcal{L} = \{S, K, Q\}$ where S, K, and Q represent the set of stations, scheduled trains during the optimization period, and power supply zones, respectively. As shown in Figure 1, for a two-way metro line with S stations ($s_i \in S$, $1 \le s_i \le s+1$), during the optimization period, K trains ($k_i \in K$, $1 \le k_i \le K$) are scheduled to run according to passenger demand [origin-destinations (ODs)], and the trains run back and forth to serve the passengers in a stop-and-go manner. The train traction power is provided by Q power supply zones ($q_i \in Q$, $1 \le q_i \le q$), and the train adopts energy-saving strategies while in operation. The dissipative regenerative braking energy can be used by up-and-down trains operating within the same power supply zone, and its utilization efficiency is affected by the synergy of multiple trains' control conditions. To ensure an adequate service and promote energy conservation, the trains were operated in a non-parallel mode. Given the constraints of meeting passenger demands and train operation requirements, the optimization objectives were set to achieve the minimum cost of passenger travel and the minimum net energy consumption of train operations. The optimized energy-saving timetable was created by determining the dwell and headway times of each train at each station, as well as the running time and control conditions of each section, finally leading to an optimized energy-saving timetable.

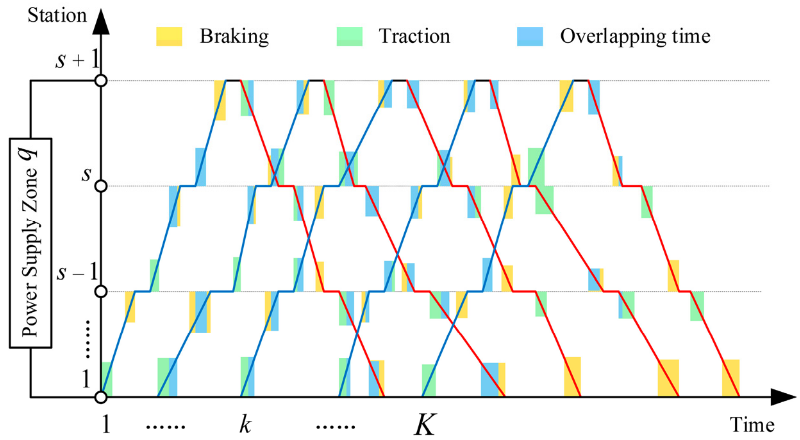

Figure 1. Schematic diagram of energy saving by multi-train non-parallel operation cooperation.

3.1. Symbols and Variables

3.1.1. Symbol Definition

Define the station set $ST = \{1, 2, 3, \cdots, 2S\}$ and station index $s \in ST$, and stipulate that the index of the first up-direction station is 1 and the index of the first down-direction station is $S + 1$. The section set is $SE = \{1, 2, 3, \cdots, S - 1, S + 1, \cdots, 2S - 1\}$; the section index is $m \in SE$; and the length of the section m is X_m km. The power supply zone set is $PO = \{1, 2, 3, \cdots, Q\}$ and the power supply zone index is $q \in PO$. The train set $TR = \{1, 2, 3, \cdots, K\}$; the train index is $k \in TR$. The optimization period $[t_s, t_e]$ is divided into N subdivision periods with time step Δt. The subdivision period set is $TN = \{1, 2, 3, \cdots, N\}$, the subdivision period index is $n \in TN$, and the subdivision period timestamp set is $T = \{t_s, t_s + \Delta t, \cdots, t_s + N\Delta t\}$.

3.1.2. Decision Variable

Because the trains were allowed to run in a non-parallel mode, three sets of decision variables were set: the running time RT_m^k of train k along interval m, the dwell time DT_s^k of train k at station s, and the headway time h_s^k between trains k and $k-1$ when each one left station s. These three decision variables could later be converted to calculate the optimal arrival and departure times of each train at each station.

3.2. Objective Function

To maintain adequate service levels while also conserving as much energy as possible, this paper considered both the temporal and spatial distribution characteristics of dynamic passenger flows, the optimal speed profiles for train operations between two stations, and the effective utilization of regenerative braking energy through multi-train cooperation. Hence, this study set the minimum passenger travel cost and minimum net energy consumption of train operations as the optimization objectives, as described in Equations (1)–(7).

3.2.1. Passenger Travel Cost

The most effective way to reduce the cost of passenger travel time while also improving the quality of the train's service was to minimize the total travel time of the passengers. The total passenger travel time T_{tra} consisted of two parts: the waiting time T_w at the station and the traveling time T_o in the car. The specific calculation is performed as follows:

$$min\ T_{tra} = T_w + T_o \tag{1}$$

$$T_w = \sum_{k=1}^{K} \sum_{s=1}^{S} ((P_{s,k}^{arr} \cdot \frac{h_s^k}{2} + P_{s,k-1}^{str} \cdot h_s^k) \cdot h_s^k) \tag{2}$$

$$T_o = \sum_{k=1}^{K}\sum_{s=1}^{S}\left(P_{s,k}^{in}\cdot RT_m^k + (P_{s,k}^{in} - P_{s+1,k}^{ali})\cdot DT_{s+1}^k\right) \quad (3)$$

where $P_{s,k}^{arr}$ represents the number of passengers who access the platform and wait for train k at the time when train $k-1$ leaves station s; $P_{s,k}^{str}$ gives the number of passengers stranded on the platform when train k leaves station s. Meanwhile, $P_{s,k}^{in}$ indicates the number of passengers aboard train k when it leaves station s; $P_{s,k}^{ali}$ is the number of passengers who alight from train k when it stops at station s.

3.2.2. Net Energy Consumption

With the utilization of regenerative braking energy, each train consumes both traction power supply energy and regenerative braking energy during its operation. In the research subdivision period n, the traction energy consumption $E_q^A(t)$ and regenerative braking energy $E_q^B(t)$ for the power supply zone q can each be calculated using Equations (4) and (5):

$$E_q^A(t) = \sum_{k=1}^{TR}\sum_{m=1}^{SE} F_{m,k}(t)\cdot v_{m,k}(t)\cdot \varphi_{m,q} \quad (4)$$

$$E_q^B(t) = \begin{cases} \sum\limits_{k=1}^{TR}\sum\limits_{m=1}^{SE} B_{m,k}(t)\cdot v_{m,k}(t)\cdot \varphi_{m,q}\cdot\lambda & v_{m,k}(t) > v_e \\ 0 & v_{m,k}(t) \le v_e \end{cases} \quad (5)$$

where $F_{m,k}(t)$ and $B_{m,k}(t)$ represent the traction and braking forces, respectively; $v_{m,k}(t)$ is the speed of train k running along section m at time t; and $\varphi_{m,q}$ is a binary variable. If section m belongs to the power supply zone q, $\varphi_{m,q} = 1$; otherwise, $\varphi_{m,q} = 0$. In addition, λ is the conversion efficiency of the regenerative braking energy; v_e is the critical speed of regenerative braking and air braking, and the regenerative braking energy can be generated only when $v_{m,k}(t) > v_e$.

If the regenerative braking energy is not used in time, its surplus energy is dissipated by the resistor in the form of heat energy. In this paper, the principle of "minimum utilization" was adopted to calculate the quantity of regenerative braking energy utilized during the research subdivision period:

$$E_q^{BU}(t) = min\left\{E_q^A(t), E_q^B(t)\right\} \quad (6)$$

The net energy consumption for the train's operation is the differential value between the total traction energy consumption and the quantity of regenerative braking energy utilized. Thus, the net energy consumption for the train's operation can be expressed as shown in Equation (7):

$$minE = \sum_{q=1}^{Q}\sum_{n=1}^{N}\sum_{t\in n}\left[E_q^A(t) - E_q^B(t)\right] \quad (7)$$

3.3. Constraints

3.3.1. Constraints of Train Force and Motion

The calculation of the net energy consumption level in the objective function highlights the impact of multi-train cooperations on energy efficiency. Consequently, it is important to facilitate the effective cooperation among trains along the section, while adhering to the prescribed energy-saving strategies and timetables. In this study, we used the three-stage optimal control strategy [9] of "traction–coasting–braking", as shown in Figure 2, and then set the train force and motion equation constraints.

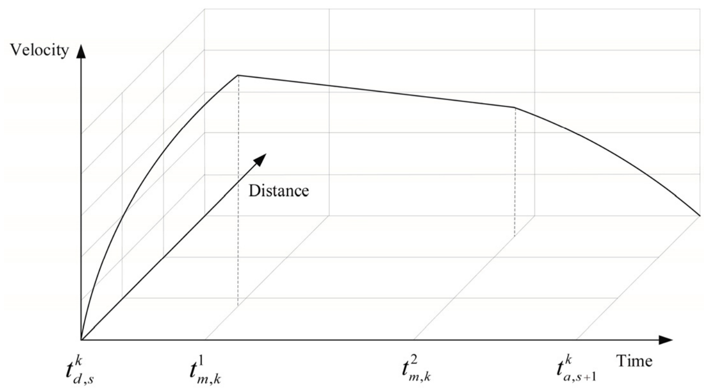

Figure 2. Schematic diagram of three-stage optimal speed curve.

Train Force Constraints: train operation is primarily affected by the traction force, braking force, and basic resistance. Basic resistance can be calculated according to the following empirical equation [13]:

$$R_{m,k}(t) = M_{m,k}\left(a + bv_{m,k}(t) + cv^2_{m,k}(t)\right) \tag{8}$$

where $R_{m,k}(t)$ is the basic resistance, while a, b, and c are the basic resistance coefficients and $M_{m,k}$ is the train mass. For train k running along section m, if the average passenger mass is m_p and the empty train mass is M_t, the train mass $M_{m,k}$ can be expressed as:

$$M_{m,k} = M_t + P^{in}_{s,k} \cdot m_p \tag{9}$$

According to Newton's second law of motion, the combined force on the train speed curve at each stage is:

$$C_{m,k}(t) = (1+\rho)M_{m,k}\frac{dv_{m,k}(t)}{dt} = \begin{cases} F_{m,k}(t) - R_{m,k}(t) & t \in \left[t^k_{d,s}, t^1_{m.k}\right) \\ -R_{m,k}(t) & t \in \left[t^1_{m.k}, t^2_{m.k}\right) \\ -B_{m,k}(t) - R_{m,k}(t) & t \in \left[t^2_{m.k}, t^k_{a,s+1}\right) \end{cases} \tag{10}$$

where $C_{m,k}(t)$ is the combined force on the train, and $F_{m,k}(t)$ and $B_{m,k}(t)$ represent the traction and braking forces, respectively. In addition, ρ is the coefficient of the gyration quality; $t^k_{a,s}$ and $t^k_{d,s}$ are the times at which train k arrives at and departs from station s, respectively. Finally, $t^1_{m.k}$ and $t^2_{m.k}$ indicate the moments during the operation of train k along section m at which traction turns to coasting and coasting turns to braking, respectively.

To ensure the comfort of the passengers, the train control strategy prioritizes the maximum traction and braking force. When the limit of maximum acceleration and deceleration is exceeded, the train runs at the maximum allowable acceleration and deceleration, and the constraints of the traction and braking forces of the train are expressed as follows:

$$F_{m,k}(t) = \begin{cases} \min\left[F^{max}_{m,k}, (1+\rho)M_{m,k}\alpha + R_{m,k}(t)\right] & t \in \left[t^k_{d,s}, t^1_{m.k}\right) \\ 0 & otherwise \end{cases} \tag{11}$$

$$B_{m,k}(t) = \begin{cases} \min\left[B^{max}_{m,k}, -(1+\rho)M_{m,k}\beta - R_{m,k}(t)\right] & t \in \left[t^2_{m.k}, t^k_{a,s+1}\right) \\ 0 & otherwise \end{cases} \tag{12}$$

where $F^{max}_{m,k}$ and $B^{max}_{m,k}$ indicate the maximum traction and braking forces, respectively; α and β represent the maximum acceleration and deceleration values, respectively.

Train Motion Equation Constraints: given the train stress analysis mentioned above, we regarded the train as a single-point model. From this, it followed that the train ran at a constant acceleration during time step Δt. The speed, displacement, and acceleration of the train can then be calculated according to the following train dynamics equation:

$$\begin{cases} v_{m,k}(t+\Delta t) = v_{m,k}(t) + a_{m,k}(t)\Delta t \\ x_{m,k}(t+\Delta t) = x_{m,k}(t) + \frac{v_{m,k}^2(t+\Delta t) - v_{m,k}^2(t)}{2a_{m,k}(t)} \\ a_{m,k}(t) = \frac{dv_{m,k}(t)}{dt} = \frac{C_{m,k}(t)}{(1+\rho)M_{m,k}} \end{cases} \tag{13}$$

where $x_{m,k}(t)$ denotes the running distance of the train at time t, and $a_{m,k}(t)$ provides the acceleration value of the train at time t.

The motion equation constraints that the train needs to meet can then be summarized as follows:

$$\begin{cases} v\left(t_{d,s}^k\right) = v\left(t_{a,s+1}^k\right) = 0 \\ x\left(t_{a,s+1}^k\right) - x\left(t_{d,s}^k\right) = X_m \\ t_{d,s}^k < t_{m.k}^1 < t_{m.k}^2 < t_{a,s+1}^k \\ v_{m,k}(t) \le v_{lim} \end{cases} \tag{14}$$

3.3.2. Constraints of Train Capacity and Passenger Boarding and Alighting

With the constraints on the motion of the train already calculated, we then turned to defining the constraints on train capacity and passenger flow.

$$P_{s,k}^{arr} = \left(t_{d,s}^k - t_{d,s}^{k-1}\right) \cdot \eta_{s,k},\ t_{d,s}^k \in n \tag{15}$$

$$P_{s,k}^{w} = P_{s,k}^{arr} + P_{s,k-1}^{str} \tag{16}$$

$$P_{s,k}^{in} = P_{s-1,k}^{in} + P_{s,k}^{boa} - P_{s,k}^{ali} \tag{17}$$

$$P_{s,k}^{ali} = P_{s-1,k}^{in} \cdot \mu_{s,k} \tag{18}$$

$$P_{s,k}^{boa} = min\left\{\left(P_{cap} - P_{s-1,k}^{in} + P_{s,k}^{ali}\right), P_{s,k}^{w}\right\} \tag{19}$$

$$P_{s,k}^{str} = P_{s,k}^{w} - P_{s,k}^{boa} \tag{20}$$

where $\eta_{s,k}$ represents the rate of arrival of passengers at station s during the study period; $P_{s,k}^{w}$ is the number of passengers waiting to board at the platform when train k arrives at station s; $P_{s,k}^{boa}$ is the number of boarding passengers when train k passes through station s; and $P_{s,k}^{ali}$ denotes the number of passengers that alight when train k passes through station s. Finally, $\mu_{s,k}$ presents the ratio of passengers who alight to passengers remaining aboard when train k arrives at station s.

More specifically, in this set of calculations, Equation (16) determines the actual passenger flow demand, while Equation (19) indicates that the number of boarding passengers depends on both the available capacity of train k and the boarding demand at station s. Equation (20), meanwhile, calculates the train capacity constraint.

3.3.3. Constraints of the Train Operation Interval

The final set of constraints we had to determine were the restrictions on the intervals at which trains could operate along section m.

$$h_{min} \le h_s^k \le h_{max} \tag{21}$$

$$RT_{min}^m \le RT_m^k \le RT_{max}^m \tag{22}$$

$$DT^s_{min} \leq DT^k_s \leq DT^s_{max} \tag{23}$$

where Equation (21) represents the headway time constraint, which ensures a safe distance between the front and rear trains. In this expression, h_{min} and h_{max} denote the lower and upper limits of the headway time necessary for the safe operation of the trains. Equation (22) limits the section running time, where RT^m_{min} and RT^m_{max} are the minimum and maximum running times allowed for the section; Equation (23) specifies the upper and lower (DT^s_{min} and DT^s_{max}, respectively) limits of the train dwell time. All notations of the mentioned symbols, variables, and parameters are shown in Table A1 in the Appendix A.

4. Heuristic Algorithm

4.1. Algorithm Framework

The model constructed in this paper had multiple optimization objectives and decision variables, with the numerous and interrelated constraints typical of an NP-hard problem. Most current research aims to solve a multi-objective train timetable problem, which is usually converted into a single-objective problem and solved using commercial solver CPLEX [27] or another intelligent algorithm [26]. In order to preserve the diversity of solutions, this paper designed a multi-objective evolutionary algorithm based on the NSGA-II algorithm through Python [28]. This caused the optimization results to converge along a Pareto frontier. The algorithm framework is shown in Figure 3 and the specific steps of the algorithm's design are described below in the following sections.

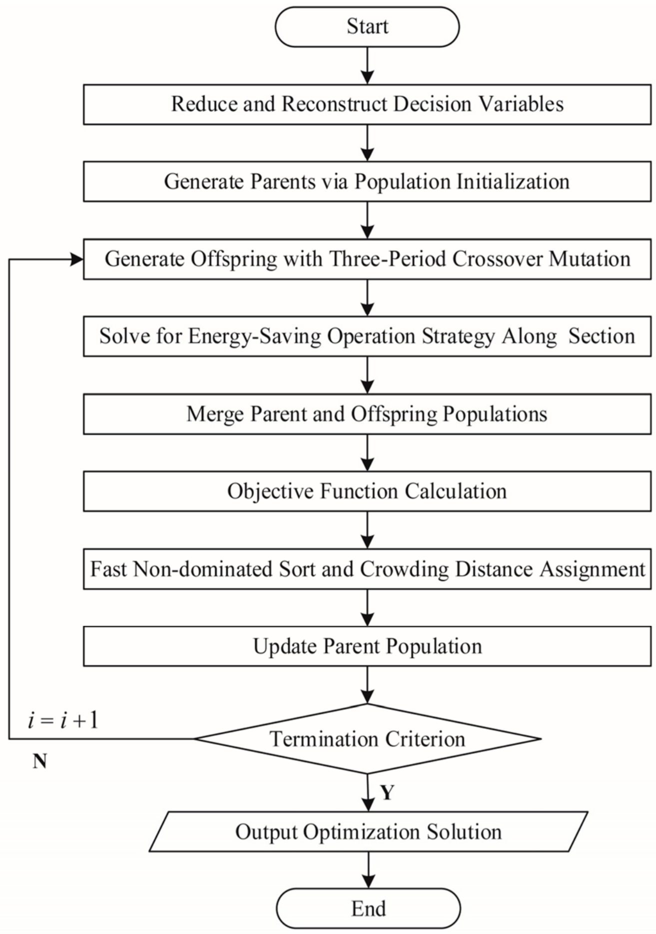

Figure 3. Multi-objective evolutionary algorithm flow.

4.2. Reduce and Reconstruct Decision Variables

Because of the non-parallel running of trains, the abovementioned model needed to optimize the trajectories of all trains within the optimization period. At present, there are too many decision variables, making a solution difficult. We designed the mechanism of "Train Grouping and Non-parallel Operation" and "Train Location-Time Tracking" to reduce the number of decision variables.

Definition 1. *"Train Grouping and Non-parallel Operation" refers to the formation of a Train Group comprising several adjacent trains. Trains in the same Train Group run in parallel, while trains in different groups do not run in parallel.*

With the introduction of the Train Group, the headway time can be reduced to two arrays, namely, array H between Train Groups and array $\hat{H}$ within Train Groups. If NK is defined as the number of Train Groups, then H and $\hat{H}$ can be expressed as:

$$H = (h_1, h_2, \cdots, h_{NK-1})_{1\times(NK-1)}$$

$$\hat{H} = \left(\hat{h}_1, \hat{h}_2, \cdots, \hat{h}_{NK}\right)_{1\times NK}$$

Definition 2. *"Train Location-Time Tracking" refers to the discrete value combination sequence of the dwell and inter-station running times of the first train of a Train Group in a station segment. This allows us to reduce the dwell and inter-station running times of all trains to the Train Location-Time Tracking array LT, which is expressed as:*

$$LT = \begin{pmatrix} lt_1^1 & lt_2^1 & \cdots & lt_{2NS}^1 \\ lt_1^2 & lt_2^2 & \cdots & lt_{2NS}^2 \\ \vdots & \vdots & \vdots & \vdots \\ lt_1^{NK} & lt_2^{NK} & \cdots & lt_{2NS}^{NK} \end{pmatrix}_{NK\times 2NS}$$

where lt_j^i indicates the Location-Time Tracking of the first train in Train Group i to arrive at station location j, with NS representing the number of one-way station segments.

Following the dimensionality reduction and reconstruction, the decision variables comprise array LT, headway time array $\hat{H}$, and headway time array H, and are expressed as follows:

$$\left(lt_1^1, lt_2^1, \cdots, lt_{2NS}^1, lt_1^2, \cdots, lt_1^{NK}, \cdots, lt_{2NS}^{NK}, \hat{h}_1, \hat{h}_2, \cdots, \hat{h}_{NK}, h_1, h_2, \cdots, h_{NK-1}\right) \quad (24)$$

4.3. Generate Parents via the Population Initialization

Sub-algorithm I was designed to generate an initial solution to the combination of decision variables described in Equation (24). The specific steps are as follows:

Sub-Algorithm I: Initial Solution Generation

Step 1: Assign the initial departure time of the first train in the first Train Group, and set $i = 1$;

Step 2: Randomly select $lt_1^i, lt_2^i,, \cdots, lt_{2NS}^i$, and $\hat{h}_{\mathrm{i}}$;

Step 3: $i = i + 1$; if $i \leq NK$, go to Step 4; otherwise, go to Step 6;

Step 4: Randomly select $\hat{h}_i$ and h_i;

Step 5: Let $j = 1$;

Step 5.1: Randomly select lt_j^i; check and adjust the headway times between the first train in Train Group i and the last train in Train Group $i - 1$;

Step 5.2: $j = j + 1$; if $j \leq 2NS$, return to Step 5.1; otherwise, go to Step 3;

Step 6: The algorithm ends and the initial solution is output.

4.4. Generate Offspring via the Three-Period Crossover Mutation

Sub-algorithm II realized $\left(LT \rightarrow H \rightarrow \hat{H}\right)$ using a three-period crossover mutation to generate offspring. Specifically, it used LT crossover→LT mutation→H crossover→H mutation→$\hat{H}$ crossover→$\hat{H}$ mutation to generate offspring. The steps are given below:

Sub-Algorithm II: Generating Offspring via the Three-Period Crossover Mutation

Step 1: Select individuals from parent population P according to the LT crossover ratio R_{ltc}; perform crossover operations on the selected individuals according to the number of LT crossover station segments N_{ltc};

Step 2: Select individuals from parent population P according to the LT mutation ratio R_{ltm}; perform mutation operations on the selected individuals according to the number of LT mutation train groups $N_{ltm,1}$ and the number of LT mutation station segments $N_{ltm,2}$;

Step 3: Select individuals from parent population P according to the H crossover ratio R_{hoc}; perform crossover operations on the selected individuals according to the number of H crossover train groups N_{hoc};

Step 4: Select individuals from parent population P according to the H mutation ratio R_{hom}; perform mutation operations on the selected individuals according to the number of H mutation train groups N_{hom};

Step 5: Select individuals from parent population P according to the $\hat{H}$ crossover ratio R_{hic}; perform crossover operations on the selected individuals according to the number of $\hat{H}$ crossover train groups N_{hic};

Step 6: Select individuals from parent population P according to the $\hat{H}$ mutation ratio R_{him}; perform mutation operations on the selected individuals according to the number of $\hat{H}$ mutation train groups N_{him}.

After each crossover or mutation, the departure time of the relevant train groups from the first station must be adjusted to ensure that the calculated headway time meets the model constraints.

4.5. Solve for Energy-Saving Train Operation Strategies

On the basis of the feasible solutions generated above, sub-algorithm III calculates the optimal energy-saving operation strategy for trains over different track sections. The specific steps are as follows:

Sub-Algorithm III: Determining Energy-Saving Train Operation Strategies

Step 1: Forward deduce the maximum traction curve, that is, the curve of a vehicle accelerating from 0 to v_{lim}; the time when $v = v_{lim}$ is t_{lim};

Step 2: Deduce in reverse the maximum braking curve, that is, the curve of a vehicle decelerating from v_{lim} to 0;

Step 3: Find the minimum coasting time δ_{min};

Step 3.1: Let $\delta = 2$ s and draw the traction–coasting curve. The velocity at time t_e is v_e, and if $v_e \geq 0$, $\delta_{min} = 2$ s, then go to Step 4; if $v_e < 0$, go to Step 3.2;

Step 3.2: Let $\delta = \frac{t_{lim}}{2}$, draw the traction–coasting curve, and record v_e;

Step 3.3: If $v_e = 0$ and $\delta_{min} = \delta$, proceed to Step 4; otherwise, go to Step 3.4;

Step 3.4: If $v_e > 0$, let $\delta = \frac{\delta+0}{2}$; if $v_e < 0$, let $\delta = \frac{\delta+t_{lim}}{2}$. Draw the traction–coasting curve under the new δ, calculate v_e, and return to Step 3.3;

Step 4: The distance between the stations is X_m. Calculate the distance $X_m{}'$ traveled by the train when $\delta = \frac{\delta_{min}+t_{lim}}{2}$;

Step 4.1: If $X_m{}' = X_m$, δ is the coasting start time; proceed to Step 5. Otherwise, go to Step 4.2;

Step 4.2: If $X_m{}' > X_m$, let $\delta = \frac{\delta+\delta_{min}}{2}$; if $X_m{}' < X_m$, let $\delta = \frac{\delta+t_{lim}}{2}$. Calculate $X_m{}'$ under the new δ and return to Step 4.1;

Step 5: At this time, the δ value obtained is the coasting start time. Draw the traction–coasting curve;

Step 6: Find the intersection ω of Steps 5 and 2, i.e., the transition point between coasting and braking. Then, find the complete three-stage energy-saving speed curve.

5. Numerical Experiment

5.1. Case Description

In this section, we applied the proposed optimization method to the data collected from the Yizhuang Line of the Beijing metro and explored the effectiveness of three different schemes through Python. The collected data included the set of stations, scheduled trains during the optimization period, power supply zones, and relevant parameters (e.g., energy consumption and passenger flow). The Yizhuang Line is a two-way subway line with a total length of 23.3 km, comprising 13 stations and 12 running sections. The trains travel upward from Ciqu Station (CQ) to Songjiazhuang Station (SJZ). The whole line is divided into six power supply zones, and trains operating in both directions in the same power supply zone share a substation. Table 1 summarizes the specific line data. The line uses DKZ32 trains, and the relevant train operation parameters are shown in Table 2. The dwell time and passenger flow data at the stations between 7:30 and 9:30 (the morning peak period of a typical working day) are recorded in Table 3.

Table 1. Description of the Yizhuang Line of the Beijing metro system in China.

Section	Power Supply Zone	Length (m)	Speed Limit (km/h)	Running Time Range (s)
SJZ-XC	1	2641	80	[150, 210]
XC-XHM	2	1337	80	[90, 150]
XHM-JG	2	2377	80	[140, 180]
JG-YZQ	3	1993	80	[120, 180]
YZQ-YZWHY	3	998	80	[70, 120]
YZWHY-WYJ	3	1543	80	[100, 150]
WYJ-RJDJ	4	1285	80	[90, 150]
RJDJ-RCDJ	4	1360	80	[90, 150]
RCDJ-TJNL	5	2348	80	[140, 180]
TJNL-JHL	5	2274	80	[130, 180]
JHL-CQN	6	2096	80	[120, 180]
CQN-CQ	6	1290	80	[90, 150]
Turnaround	—	—	—	90

Note: The task of turnaround is the process in which trains reverse their direction at the end of the line, which has no specific power supply zone, line length and speed limit. However, it is expected that the train completes this task within 90 s.

Table 2. Notation of parameters.

Parameters	Description	Unit	Value	Equation
M_t	Empty train mass	kg	1.99 × 105	Equation (9)
m_p	Average passenger mass	kg	60	Equation (9)
v_e	Critical speed of regenerative braking and air braking	km/h	5	Equation (5)
α	Maximum acceleration	m/s^2	1	Equation (11)
β	Maximum deceleration	m/s^2	1	Equation (12)
$F_{m,k}^{max}$	Maximum traction force	kN	310	Equation (11)
$B_{m,k}^{max}$	Maximum braking force	kN	260	Equation (12)
h_{max}	Upper limit of headway time	s	540	Equation (21)

Table 2. *Cont.*

Parameters	Description	Unit	Value	Equation
h_{min}	Lower limit of headway time	s	70 s	Equation (21)
Δt	Time step	s	1	All Equations
P_{cap}	Passenger capacity	persons	1440	Equation (9)
λ	Conversion efficiency of regenerative braking energy	N.A.	0.8	Equation (5)
a, b, c	Basic resistance coefficients	N.A.	[1.244, 1.45 $\times$ 10^{-2}, 1.36 $\times$ 10^{-4}]	Equation (8)
ρ	Coefficient of gyration quality	N.A.	0.06	Equation (10)

Table 3. Ranges of dwell times and passenger flow data from the Yizhuang Line (upward and downward).

Station	Range of Dwell Time (s)	Upward		Downward	
		Arrival Rate	Alighting Rate	Arrival Rate	Alighting Rate
SJZ	[30, 90]	0	1	0.99	0
XC	[30, 90]	0.01	0.47	0.89	0.01
XHM	[30, 90]	0.13	0.26	0.57	0.07
JG	[30, 90]	0.68	0.42	1.11	0.31
YZQ	[30, 90]	0.36	0.20	0.54	0.13
YZWHY	[30, 90]	0.34	0.11	0.33	0.12
WYJ	[30, 90]	0.60	0.16	0.39	0.23
RJDJ	[30, 90]	0.49	0.11	0.25	0.18
RCDJ	[30, 90]	0.68	0.10	0.18	0.29
TJNL	[30, 90]	0.55	0.07	0.11	0.30
JHL	[30, 90]	0.58	0.06	0.06	0.40
CQN	[30, 90]	0.36	0.02	0.01	0.37
CQ	[30, 90]	0.60	0	0	1

5.2. Experimental Schemes

We used the data from the Yizhuang Line to verify the validity of the model and algorithms by designing three experimental timetables. We could then compare and analyze the optimization effects of these three timetables when the trains ran in parallel and non-parallel modes.

Scheme 1: The Multi-Objective (MOT) Timetable was constructed to minimize both the passenger travel time and net energy consumption by trains operating in non-parallel fashion. The station segments were divided according to the power supply zone, and three trains formed a Train Group. The crossover mutation parameters of the multi-objective evolutionary algorithm are set as shown in Table 4.

Scheme 2: The Travel-Oriented (TOT) Timetable assumed a parallel operation and used the minimum passenger travel time as the optimization goal. This scheme used the lower limits of the parameter values recorded in Tables 1 and 3 for the inter-station running and dwell times of all the trains. This timetable prioritized the travel needs of passengers without considering the net energy consumption levels. The departure interval of the TOT timetable was then obtained by an optimization.

Table 4. Notation of crossover mutation parameters.

Parameters	Description	Value
N_e	Generation	20
N_p	Population size	50
R_{ltc}	*LT* crossover ratio	50%
N_{ltc}	Number of *LT* crossover station segments	1
R_{ltm}	*LT* mutation ratio	20%
$N_{ltm,1}$	Number of *LT* mutation Train Groups	1
$N_{ltm,2}$	Number of *LT* mutation station sections	1
R_{hoc}	*H* crossover ratio	40%
N_{hoc}	Number of *H* crossover Train Groups	1
R_{hom}	*H* mutation ratio	10%
N_{hom}	Number of *H* mutation Train Groups	1
R_{hic}	$\hat{H}$ crossover ratio	20%
N_{hic}	Number of $\hat{H}$ crossover Train Groups	1
R_{him}	$\hat{H}$ mutation ratio	10%
N_{him}	Number of $\hat{H}$ mutation Train Groups	1

Scheme 3: The Energy-Oriented (EOT) Timetable also assumed a parallel operation and focused on energy savings. This scheme used the upper limits of the parameter values recorded in Tables 1 and 3 for the inter-station running and dwell times of all the trains. This reduced the traction time, increased the time spent coasting, reduced energy consumption, and allowed the calculation of the departure interval for the EOT timetable.

5.3. Results and Discussion

The analysis of the three experimental timetables, which were proposed to verify the optimization method, demonstrated the convergence and selectivity of the optimal solutions to the multi-objective evolutionary algorithm.

5.3.1. Algorithm Convergence

In Figure 4, the gray scatter plot shows the target values of the last generation of the MOT optimization solution obtained after five iterations of the experiment. The distribution of the optimization solutions allows us to derive the Pareto frontier with the shortest passenger travel time and the lowest net energy consumption level, as shown by the dotted line in Figure 4. The blue and green scatter dots correspond to the net energy consumption levels and travel times associated with the optimal TOT and EOT solutions, respectively. These ten departure intervals, located at the extremes of the Pareto frontier, indicate the scientific and excellent performances of the model and the multi-objective evolutionary algorithm developed in this study, in terms of both the convergence and optimization.

5.3.2. Solution Comparison

In Figure 4, it can be observed that the MOT solutions are not densely clustered along the Pareto front. To analyze the differences between the optimization solutions, four parameters were selected for comparison: the number of departure trains at the first station, the converted number of departure trains, the number of passengers served, and the utilization ratio of the regenerative braking energy. Here, the converted train number represents the ratio of the number of stations that the train passes through during the optimization period to the number of total stations.

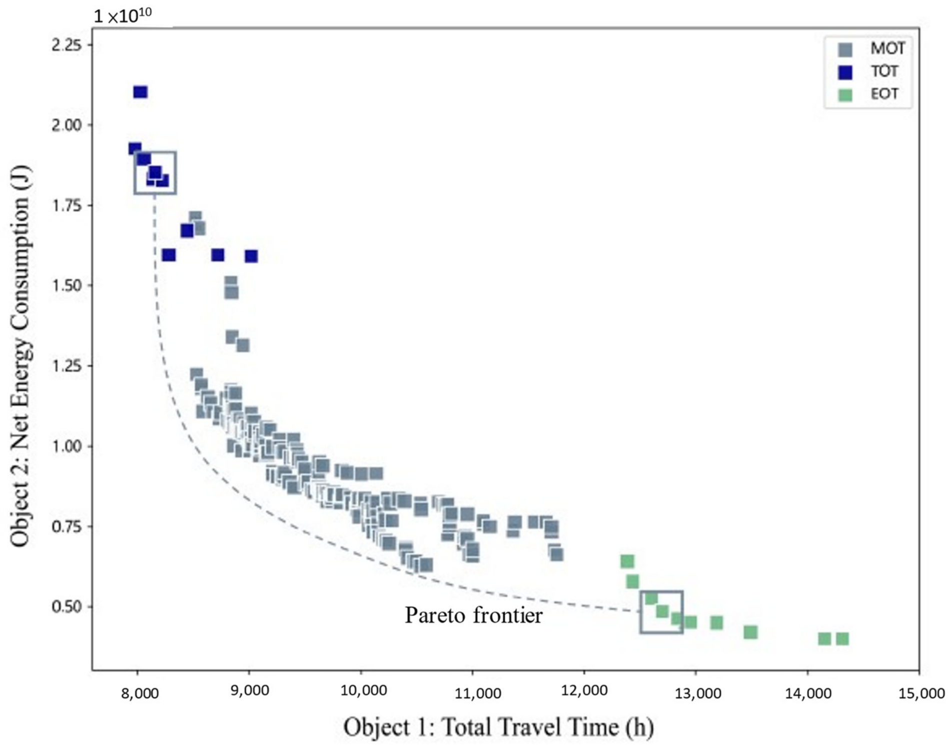

Figure 4. Distribution of optimal solutions and the Pareto frontier.

Figure 5 shows the distribution characteristics of the reduced number of departure trains and the utilization ratio of the regenerative braking energy when the travel time ranges between 8000 and 12,000. The figure is divided into four quadrants, using the converted number of departure trains (14) and the travel time (10,000 h) as reference points. In Quadrant I, the converted number of departure trains is greater, and the passenger travel time is longer, leading to a lower distribution of optimal solutions. Due to two objectives in the proposed model, the diversified optimization solutions are distributed throughout Quadrants II, III, and IV. This allows operation managers to choose from these solutions based on their preferences and requirements.

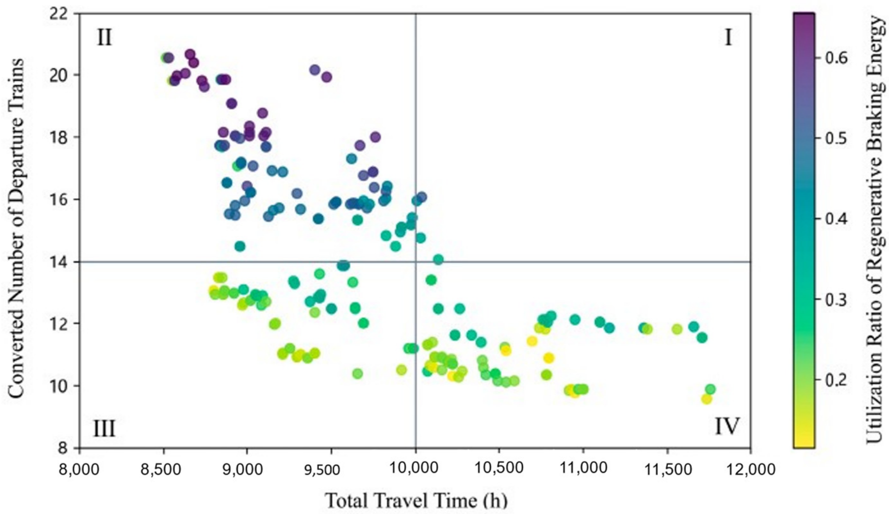

Figure 5. Relation diagram of the optimized solutions.

In Quadrant III, the utilization ratio of regenerative braking is lower than that in Quadrant II when the converted number of departure trains is lower, and the passenger travel time is shorter. However, in a constant optimization period, the rise in the converted number of departure trains represents an increase in the traction energy consumption level. As a result, the net energy consumption of the optimization solutions in Quadrant III is basically the same as that in Quadrant II. Additionally, Figure 6 presents additional data on the number of passengers served by different converted numbers of departure trains in Quadrant III. It is important to note that the MOT satisfactory solution serves the largest number of passengers among all solutions.

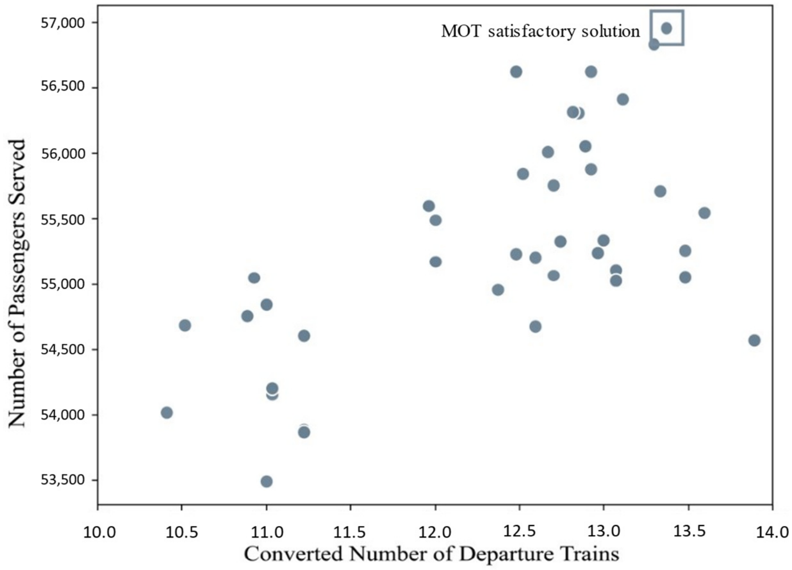

Figure 6. Relation diagram of passengers served by the converted number of departure trains.

In Figure 6, the number of passengers served by the MOT satisfactory solution is 56,955, and the total travel time of passengers is 9275.74 h. The converted number of departure trains in this scenario is 13.37 and the number of departure trains at the first station is 20. As for the energy consumption level, the utilization ratio of regenerative braking energy is 29.88% and the net energy consumption level of train operations is 1.02×10^7 KJ. These calculations yield the timetable as shown in Figure 7. The optimization results of the abovementioned MOT satisfactory solution, as well as the optimal TOT and EOT departure intervals, are recorded in Table 5.

Table 5. Performance comparison of MOT, TOT, and EOT.

	MOT	TOT	EOT
Utilization ratio of regenerative braking energy	29.88%	7.28%	11.77%
Net energy consumption ($\times 10^7$ KJ)	1.02	1.85	0.46
Number of passengers served	56,955	61,667	52,615
Total travel time of passengers (h)	9275.74	8157.90	12,738.48

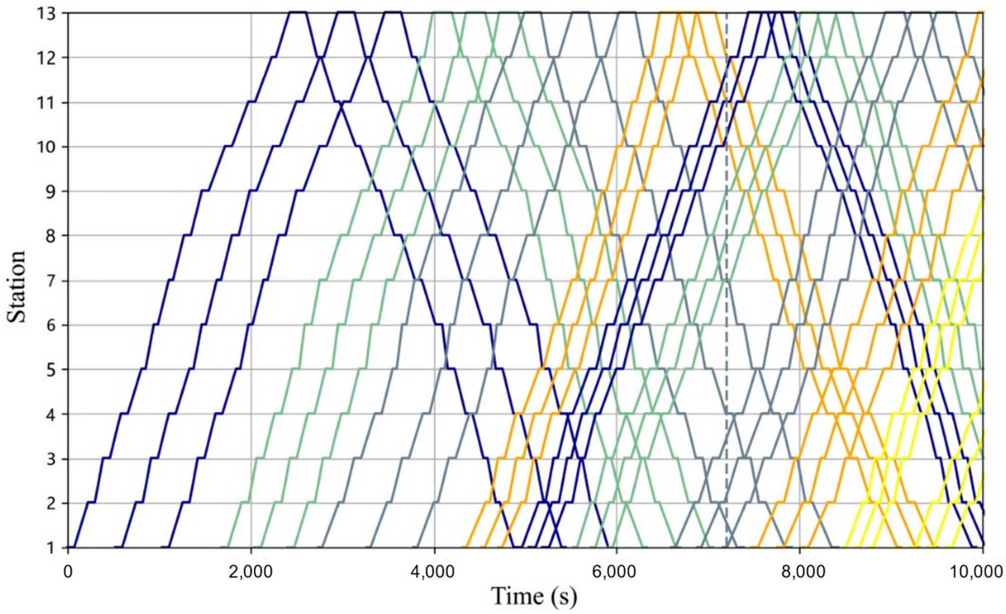

Figure 7. MOT satisfactory solution.

Table 5 highlights that the TOT yields the shortest total travel time for passengers, while the EOT minimizes net energy consumption levels, which aligns with the initial definitions of these two timetables. The MOT satisfactory solution presented in this study effectively enhanced the utilization ratio of regenerative braking energy through the non-parallel train operations. Compared to the TOT, the MOT satisfactory solution reduced the net energy consumption by 44.86%, considerably reducing the power consumption of the train system. Furthermore, compared to the EOT, the MOT satisfactory solution lowered the total travel time of passengers by 27.18%, providing improved transportation options for more passengers during the same period. The original timetable of the Yizhuang Line had a regenerative braking energy utilization rate of 7.51% and a net energy consumption rate of 1.1×10^7 KJ. In contrast, the MOT satisfactory solution increased the regenerative braking energy utilization rate to 29.88% and reduced the net energy consumption rate by 20.88%.

6. Conclusions

When designing a low-carbon urban rail system, two major factors are usually considered: energy consumption and operational strategies. To ensure a good service quality while reducing the energy consumption rate, this study developed a method for optimizing an energy-saving, non-parallel operation timetable for the multi-train non-parallel operation coordination. This approach contained a multi-objective optimization model that considered both the effective utilization of regenerative braking energy under multi-train control conditions and the temporal and spatial distribution characteristics of dynamic passenger flows. This approach also developed an improved multi-objective evolutionary algorithm based on NSGA-II. An empirical case based on the Yizhuang Line of the Beijing metro allowed us to explore the feasibility of the proposed method. The simulation results show that the optimization method improves energy utilization and passenger service levels along a Pareto front. By using the MOT, the utilization of regenerative braking energy increased by 29.88% in comparison with the original timetable, while the net operational energy consumption was reduced by 44.86% compared with the TOT. In comparison to the EOT, the optimization model also reduced the total passenger travel time by 27.18%. These results confirm that the proposed optimization method effectively reduces the net energy consumption by train operations while guaranteeing a certain level of service quality. Furthermore, the improved multi-objective evolutionary algorithm provided optimal solutions that satisfied diverse preferences and objectives.

We should note that this study simplified train speed profiles between stations into only three stages (traction, coasting, and braking). The speed characteristics of each line section in the real world would be heterogenous; however, they would be influenced by measures, like cruise control, to maintain train spacing or changes in weather conditions. A bi-level optimization model would allow for a further investigation of the heterogeneity of train speed profiles. A further objective should be added (e.g., reducing the operational cost of rolling stock).

Author Contributions: W.C.: conceptualization, methodology, writing—original draft, review, and editing; J.L.: methodology, writing—original draft and editing; H.Z.: software, data analysis; Z.Y.: data analysis, writing—review, and editing. All authors have read and agreed to the published version of the manuscript.

Funding: The study is supported by the Science and Technology Program of Hunan Provincial Department of Transportation (Grant No.202225).

Data Availability Statement: Not applicable.

Acknowledgments: The authors acknowledge the data support and constructive advice provided by the Beijing Mass Transit Railway Operation Corp., Ltd.

Conflicts of Interest: The authors declare no conflict of interest. The funder had no role in the design of the study; in the collection, analyses, or interpretation of data; in the writing of the manuscript; or in the decision to publish the results.

Appendix A

Table A1. Notations of symbols, variables, and parameters.

Symbols/Variables	Description
s	Station index
m	Section index
X_m	Length of the section m
q	Power supply zone index
k	Train index
n	Subdivision period index
RT_m^k	Running time of train k along the section m
RT_{min}^m	Minimum running time allowed for the section m
RT_{max}^m	Maximum running time allowed for the section m
DT_s^k	Dwell time of train k at station s
DT_{min}^s	Upper limit of the train dwell time
DT_{max}^s	Lower limit of the train dwell time
h_s^k	Headway time between trains k and $k-1$ when each of them leaves station s
h_{min}	Lower limit of headway time necessary for the safe operation of the trains
h_{max}	Upper limit of headway time necessary for the safe operation of the trains
T_{tra}	Total passenger travel time
T_w	Waiting time at the station
T_o	Traveling time in the car
$P_{s,k}^{arr}$	Number of passengers who enter the platform and wait for train k at the time when train $k-1$ leaves station s

Table A1. *Cont.*

Symbols/Variables	Description
$P^{str}_{s,k}$	Number of passengers stranded on the platform when train k leaves station s
$P^{in}_{s,k}$	Number of passengers aboard train k when it leaves station s
$P^{ali}_{s,k}$	Number of passengers who alight from train k when it stops at station s
$\eta_{s,k}$	Rate of arrival of passengers at station s during the study period
$P^{w}_{s,k}$	Number of passengers waiting to board at the platform when train k arrives at station s
$P^{boa}_{s,k}$	Number of boarding passengers when train k passes through station s
$P^{ali}_{s,k}$	Number of passengers that alight when train k passes through station s
$\mu_{s,k}$	Ratio of passengers who alight to passengers remaining aboard when train k arrives at the station s
$E^{A}_{q}(t)$	Traction energy consumption for power supply zone q at time t
$E^{B}_{q}(t)$	Regenerative braking energy for power supply zone q at time t
$F_{m,k}(t)$	Traction force of train k running along section m at time t
$B_{m,k}(t)$	Braking force of train k running along section m at time t
$v_{m,k}(t)$	Speed of train k running along section m at time t
$R_{m,k}(t)$	Basic resistance of train k running along section m at time t
$C_{m,k}(t)$	Combined force of train k running along section m at time t
$x_{m,k}(t)$	Running distance of train k running along section m at time t
$a_{m,k}(t)$	Acceleration of train k running along section m at time t
$M_{m,k}$	Train mass of train k running along section m
$\varphi_{m,q}$	A binary variable. If sec tion m belongs to the power supply zone q, $\varphi_{m,q} = 1$; otherwise, $\varphi_{m,q} = 0$.
a, b, and c	Basic resistance coefficients
λ	Conversion efficiency of regenerative braking energy
v_e	Critical speed of regenerative braking and air braking
m_p	Average passenger mass
M_t	Empty train mass
ρ	Coefficient of gyration quality
$t^{k}_{a,s}$	Times at which train k arrives at station s
$t^{k}_{d,s}$	Times at which train k departs from station s
$F^{max}_{m,k}$	Maximum traction force
$B^{max}_{m,k}$	Maximum braking force
α	Maximum acceleration
β	Maximum deceleration

References

1. Nakamura, K.; Hayashi, Y. Strategies and instruments for low-carbon urban transport: An international review on trends and effects. *Transp. Policy* **2013**, *29*, 264–274. [CrossRef]
2. Li, Y.; He, Q.; Luo, X.; Zhang, Y.; Dong, L. Calculation of life-cycle greenhouse gas emissions of urban rail transit systems: A case study of Shanghai Metro. *Resour. Conserv. Recycl.* **2018**, *128*, 451–457. [CrossRef]
3. He, D.; Yang, Y.; Chen, Y.; Deng, J.; Shan, S.; Liu, J.; Li, X. An integrated optimization model of metro energy consumption based on regenerative energy and passenger transfer. *Appl. Energy* **2020**, *264*, 114770. [CrossRef]
4. Huang, Y.; Yang, L.; Tang, T.; Gao, Z.; Cao, F. Joint train scheduling optimization with service quality and energy efficiency in urban rail transit networks. *Energy* **2017**, *138*, 1124–1147. [CrossRef]
5. Xie, J.; Zhang, J.; Sun, K.Y.; Ni, S.Q.; Chen, D.J. Passenger and energy-saving oriented train timetable and stop plan synchronization optimization model. *Transp. Res. D Transp. Environ.* **2021**, *98*, 102975. [CrossRef]

6. Wang, P.; Goverde, R.M.P. Multi-train trajectory optimization for energy-efficient timetabling. *Eur. J. Oper. Res.* **2019**, *272*, 621–635. [CrossRef]
7. Su, S.; Li, X.; Tang, T.; Gao, Z. A subway train timetable optimization approach based on energy-efficient operation strategy. *IEEE Trans. Intell. Transp. Syst.* **2013**, *14*, 883–893. [CrossRef]
8. Alfieri, L.; Battistelli, L.; Pagano, M. Impact on railway infrastructure of wayside energy storage systems for regenerative braking management: A case study on a real Italian railway infrastructure. *IET Electr. Syst. Transp.* **2019**, *9*, 140–149. [CrossRef]
9. González-Gil, A.; Palacin, R.; Batty, P. Optimal energy management of urban rail systems: Key performance indicators. *Energy Convers. Manag.* **2015**, *90*, 282–291. [CrossRef]
10. Peng, Q.; Li, W.; Wang, Y.; Zhong, Q.; Sun, J. Study on operation strategies for metro trains under regenerative braking. *J. China Railw. Soc.* **2017**, *39*, 7–13.
11. Feng, Y.; Chen, S.; Ran, X.; Bai, Y.; Jia, W. Energy saving operation optimization of urban rail transit trains through the use of regenerative braking energy. *J. China Railw. Soc.* **2018**, *40*, 15–22.
12. Wei, R.; Du, P.; Yang, Y.; Hu, L. Analysis on Utilization of Regenerative Braking Energy for Metro Trains and Research on Timetable Optimization Method. *J. China Railw. Soc.* **2020**, *42*, 7085809.
13. Yang, Z.; Zhu, F.; Lin, F. Deep-reinforcement-learning-based energy management strategy for supercapacitor energy storage systems in urban rail transit. *IEEE Trans. Intell. Transp. Syst.* **2020**, *22*, 1150–1160. [CrossRef]
14. Peña-Alcaraz, M.; Fernández, A.; Cucala, A.P.; Ramos, A.; Pecharromán, R.R. Optimal underground timetable design based on power flow for maximizing the use of regenerative-braking energy. *Proc. Inst. Mech. Eng. Part F J. Rail Rapid Transit* **2012**, *226*, 397–408. [CrossRef]
15. Bai, Y.; Zhou, Y.; Qiu, Y.; Jia, W.; Mao, B. Energy-efficient control method for subway train in section with long heavy down grade. *China Railw. Sci.* **2018**, *39*, 108–115.
16. Zhang, L.; He, D.; He, Y.; Liu, B.; Chen, Y.; Shan, S. Real-time energy saving optimization method for urban rail transit train timetable under delay condition. *Energy* **2022**, *258*, 124853. [CrossRef]
17. Yang, X.; Li, X.; Gao, Z.; Wang, H.; Tang, T. A cooperative scheduling model for timetable optimization in subway systems. *IEEE Trans. Intell. Transp. Syst.* **2012**, *14*, 438–447. [CrossRef]
18. Lian-bo, D.; Min, Z.; Li, C.A.I. Optimization of Train Operation Strategy on An Urban Rail Section Based on Multiple Speed Parameters Control. *J. Transp. Syst. Eng. Inf. Technol.* **2021**, *21*, 111.
19. He, D.; Zhou, J.; Li, Y.; Chen, E.; Xiang, W. Energy saving optimization method for metro train based on matrix discrete method and its implementation. *J. China Railw. Soc.* **2015**, *37*, 9–14.
20. Sun, X.; Lu, H.; Dong, H. Energy-efficient train control by multi-train dynamic cooperation. *IEEE Trans. Intell. Transp. Syst.* **2017**, *18*, 3114–3121. [CrossRef]
21. Bai, Y.; Yuan, B.; Li, J.; Zhou, Y.; Feng, X. Cooperation Control Strategy for Energy Saving Operation of Metro Train Based on Rolling Optimization. *J. China Railw. Soc.* **2020**, *41*, 163.
22. Niu, H.; Zhou, X. Optimizing urban rail timetable under time-dependent demand and oversaturated conditions. *Transp. Res. Part C Emerg. Technol.* **2013**, *36*, 212–230. [CrossRef]
23. He, D.; Zhang, L.; Guo, S.; Chen, Y.; Shan, S.; Jian, H. Energy-efficient train trajectory optimization based on improved differential evolution algorithm and multi-particle model. *J. Clean. Prod.* **2021**, *304*, 127163. [CrossRef]
24. Gao, H.; Zhang, Y.; Guo, J.; Li, K.H. The two-stage optimization method of train energy-efficient operation based on dynamic programming. *J. Southwest Jiaotong Univ.* **2020**, *55*, 946–954.
25. Ran, X.; Chen, S.; Chen, L.; Jia, W. An Energy-efficient Timetable Optimization Method for Metro Operation Considering Spatial Distribution of Passenger Flow. *J. Transp. Syst. Eng. Inf. Technol.* **2020**, *20*, 103.
26. Wu, X.; Dong, H.; Chi, K.T. Multi-objective timetabling optimization for a two-way metro line under dynamic passenger demand. *IEEE Trans. Intell. Transp. Syst.* **2020**, *22*, 4853–4863. [CrossRef]
27. Hou, Z.; Dong, H.; Gao, S.; Nicholson, G.; Chen, L.; Roberts, C. Energy-saving metro train timetable rescheduling model considering ATO profiles and dynamic passenger flow. *IEEE Trans. Intell. Transp. Syst.* **2019**, *20*, 2774–2785. [CrossRef]
28. Deb, K.; Pratap, A.; Agarwal, S.; Meyarivan, T. A fast and elitist multiobjective genetic algorithm: NSGA-II. *IEEE Trans. Evol. Comput.* **2002**, *6*, 182–197. [CrossRef]